KeA1

CHINESE ROOTS
GLOBAL IMPACT

Contents lists available at ScienceDirect

Green Chemical Engineering

journal homepage: www.keaipublishing.com/en/journals/green-chemical-engineering



Article

Facile synthesis of N-doped graphene encapsulated Ni@N/C catalyst and its catalysis for highly selective semi-hydrogenation of alkynes



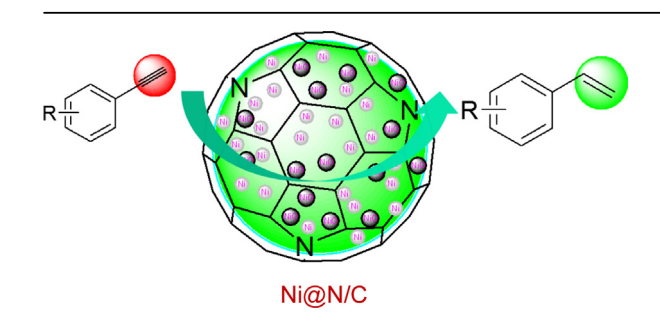
Jianguo Liu^{a,*}, Jiangmin Sun^{b,d,1}, Thishana Singh^{e,1}, Shanshan Lin^{c,d}, Longlong Ma^{a,*}

- a Key Laboratory of Energy Thermal Conversion and Control of Ministry of Education, School of Energy and Environment, Southeast University, Nanjing, 210096, China
- ^b School of Energy Science and Engineering, University of Science and Technology of China, Hefei, 230026, China
- ^c University of Chinese Academy of Sciences, Beijing, 100049, China
- ^d Guangzhou Institute of Energy Conversion, Chinese Academy of Sciences, Guangzhou, 510640, China
- ^e School of Chemistry and Physics, University of KwaZulu-Natal, Durban, 4000, South Africa

HIGHLIGHTS

- A series of N-doped graphene encapsulated Ni catalysts were synthesized *via* a facile synthesis method.
- Ni@N/C shows excellent catalytic activity for semi-hydrogenation of challenging terminal alkynes.
- The catalyst with magnetic properties has good stability and can be successfully applied in the industrial flow reactor.

GRAPHICAL ABSTRACT



ARTICLE INFO

Keywords: Graphene Nitrogen doping Ni@N/C Semi-hydrogenation Terminal alkynes

ABSTRACT

Although precious transition metals such as palladium, platinum, and iridium are widely used in hydrogenation reactions, the earth-abundant transition metal-catalyzed highly selective semi-hydrogenation of terminal alkynes to terminal alkenes remains poorly developed and a challenge. Herein we demonstrate the excellent selective, cost-effective semi-hydrogenation of terminal alkynes via a novel graphene encapsulated Ni@N/C catalyst. The graphene layer encapsulated nano-catalyst Ni@N/C could significantly avoid metal leaching and improve the stability of the catalyst. The strong interaction of nitrogen with the Ni nanoparticles regulates the activity of Ni towards selective semi-hydrogenation of terminal alkynes. Substrates having un-functionalized as well as functionalized substituents, and substrates having sensitive functional groups (olefins, ketones) which pose a challenge to hydrogenate, were semi-hydrogenated with excellent conversion (up to 99%) and selectivity (up to 99%) under optimized reaction conditions.

1. Introduction

Semi-hydrogenation of alkynes to alkenes is an important transformation in organic synthesis and has been widely used in the fine

chemical and petroleum industry [1–5]. It is well documented that alkynes are easily hydrogenated to alkenes using transition metal catalysts (Pd, Pt, Rh, Ru, Ir), however, the drawback is the presence of undesired over reduction product alkane [6–9]. In the olefin industry, alkenes are

E-mail addresses: liujg@seu.edu.cn (J. Liu), mall@seu.edu.cn (L. Ma).

https://doi.org/10.1016/j.gce.2022.01.003

Received 5 November 2021; Received in revised form 20 December 2021; Accepted 19 January 2022 Available online 24 January 2022

2666-9528/© 2022 Institute of Process Engineering, Chinese Academy of Sciences. Publishing services by Elsevier B.V. on behalf of KeAi Communication Co. Ltd. This is an open access article under the CC BY-NC-ND license (http://creativecommons.org/licenses/by-nc-nd/4.0/).

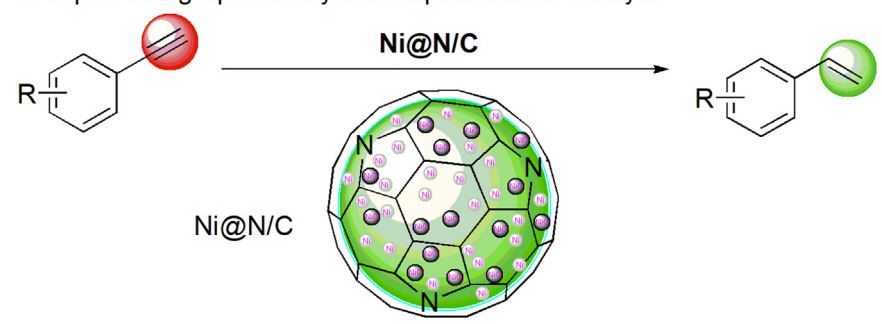
^{*} Corresponding author.

¹ These authors contributed equally to this work.

a Representative noble metal-based heterogeneous catalysts

b Representative non-noble metal-based catalysts

c N-doped thin graphene layer encapsulated Ni catalyst



Scheme 1. Heterogeneous metal-catalyzed selective hydrogenation of alkynes.

the crucial sub-starting materials for the synthesis of various valuable products like rubbers and plastics [10–12]. However, during selective hydrogenation of an alkyne to alkene, the starting material (alkyne) and the over-reduction product alkane are the harmful components that poison the subsequent alkene polymerization process. So, the development of controllable selective hydrogenation of alkynes to the alkenes, which can lower alkyne concentration and increase the desired alkene product, are of great importance [13–16].

Thus far, a variety of highly efficient transition metal catalysts have been developed and applied in the semi-hydrogenation of alkyne to the alkene. It should be noted that some of these catalysts have also been widely applied in the industry. Precious transition metals like Pd, Rh, Ir, Au are widely used in the semi-hydrogenation of internal alkynes, which usually favor Z-selectivity. Recently, the selective semi-hydrogenation of terminal alkynes, which are recognized as the more challenging substrates than internal alkynes, have been catalyzed using Pd, Au, and Ru in semi-hydrogenation, giving good to excellent catalytic activity and selectivity [3,14,17-20]. Kaneda and co-workers [21] made a significant contribution to the development of the Core-Au/Shell-CeO2 catalyst for the semi-hydrogenation of alkynes. They synthesized a novel core-shell nanocomposite Au@CeO2 catalyst using a facile co-precipitation method involving a spontaneous redox reaction between Au(III) with Ce(III) to Au(0) and Ce(IV). The core-shell structure of the catalyst can minimize the exposed Au surface sites and maximize the core-shell interface sites, thereby improving the activity and stability of the catalyst. Under mild reaction conditions (Au@CeO2 (Au: 10 mol/mol), 30-50 atm of H₂, r.t.), various alkynes including aromatic, aliphatic terminal alkynes, and internal alkynes were transformed to alkene products with good to excellent selectivity (72% \sim > 99%) (Scheme 1a). In 2017, Bao and co-workers [22] reported a heterogeneous palladium catalyst (PdNPore) for semi-hydrogenation of terminal alkynes. Under very mild reaction conditions (1 atm of H2, r.t.), ten kinds of terminal alkyne substrates including aromatic and aliphatic could be converted into corresponding terminal olefin products with a yield of 75%-88%. One equivalent of NaOH and 16–20 h reaction time was necessary for all cases (Scheme 1a). Recently, Lu et al. [14] reported a novel system having both the active metal Rh(0) and promoter ion Ga(III) on the metal-organic framework (MOF) support. The promoter Ga(III) dramatically affected the semi-hydrogenation selectivity of the Rh-Ga@NU-1000 catalyst via electronic (decreased Rh electron density and rendered it more electropositive) and structural effects (limited number of available coordination sites on Rh). Unlike the previous report, the RhGa (py3tren)@NU-1000 catalyst favored high selectivity of E-alkenes from internal alkynes, and also selectively semi-hydrogenated more than 10 terminal alkyne examples to alkenes with 80%-89% yield (Scheme 1a). A comparison of precious transition metal catalysts to earth-abundant transition metal catalysts like Fe, Co (Scheme 1b) also showed promising application in the semi-hydrogenation of alkynes, especially with regards to their low cost and bio-safety requirements [15,16,18,23-29]. Although earth-abundant transition metal homogeneous catalysts are high efficient and promising, problems such as difficulty in preparing ligands, difficult separation of products, and difficulty in reusing homogeneous catalysts restrict their wide application in industry. Moreover, the supported metal-based catalysts also suffer from active species leaching in acids or other harsh reaction conditions, which results in poor reactivity, poor stability, and selectivity in challenging synthetic organic reactions. In an attempt to solve these problems, the core-shell, yolk-shell structure catalysts encapsulate active metal nanoparticles (core) with support (shell) to maintain the high activity and stability of metals in the acidic medium was developed. These novel catalysts have recently been successfully applied in a variety of systems [30–36]. Graphene is widely used as catalyst support due to its unique properties as the thinnest and hardest material, as well as having thermal and electrical conductivity. Previously prepared graphene encapsulated catalysts had a multi-layered graphitic shell which reduced catalytic reactivity. Thus the development of advanced synthetic methods for thin graphene layers, especially twisted bilayers, three-layered graphene with superconductivity, are of great interest [37–40].

Herein, we report a facile and environmentally friendly synthesis of thin graphene shell encapsulated nitrogen doping Ni@N/C catalyst using nickel nitrate and melamine. The catalyst's chemical composition, morphology, phase structure, and its catalytic semi-hydrogenation of terminal alkynes are investigated.

2. Experimental section

2.1. Materials and analysis methods

 $Ni(NO_3)_2 \cdot 6H_2O$ (AR, 98%), anhydrous citric acid (AR, \geq 99.5%), melamine (AR, 99%), L-histidine (AR, 99%), ammonium citrate tribasic (AR, 98.5%), urea (AR, 99%), 1,2-propanediamine (AR, 99%), CDCl₃ (99.8% D, stabilized with Ag) were obtained from Shanghai Macklin Biochemical Co., Ltd.; H₂SO₄ (GR, 98%) was purchased from Sinopharm Chemical Reagent Co., Ltd.; Al₂O₃ (basic, 200-300 meshes), ethanol (AR, 99.7%), methanol (GC, > 99.9%) were purchased from Aladdin (Shanghai) Chemical Technology Co., Ltd.; Deionized water ($\sigma < 5 \,\mu\text{S m}^{-1}$) was self-made in the laboratory. Before using, the purity of aldehydes and amines has been checked. Gas Chromatography (GC) of products was recorded by GC-2014C (Shimadzu, Japan) with HP5 column (30 m \times 250 mm \times 0.25 μ m) and FID detector. Gas Chromatography-Mass Spectrometry (GC-MS) of products was determined by TRACE 1300ISQ GC-MS (Thermo Fisher Scientific, America) with TG-5MS column $(30 \text{ m} \times 250 \text{ mm} \times 0.25 \text{ } \mu\text{m})$. ¹H Nuclear Magnetic Resonance (NMR) of products were recorded on a Bruker Avance III (400 MHz) spectrometer (Bruker BioSpin, Germany) with CDCl₃ as solvent at 400 MHz. The Transmission Electron Microscope (TEM) measurements were conducted on a JEM-2100F microscope (JEOL, Japan) operated at 200 kV. The Scanning Electron Microscope (SEM) images were obtained on Analytical SEM SU-70 (Hitachi, Japan) microscope operated at 10 kV. X-ray Photoelectron Spectroscopy (XPS) measurements were performed on an Escalab250 Xi photoelectron spectrometer (Thermo Fisher Scientific, America) with Al K_{α} X-ray radiation with a scan number of 5. X-ray Diffraction (XRD) powder patterns were recorded on an X'Pert Pro MPD diffractometer (PANalytical, Netherlands) using the Cu K_{α} radiation at 40 kV and 20 mA $(\lambda = 1.5406 \text{ Å})$. Processing and assignments of the powder patterns were conducted on the software Jade 6.0 using the Powder Diffraction File (PDF) database of the International Centre of Diffraction Data (ICDD). Nitrogen adsorption isotherms were measured at $-196\,^{\circ}\text{C}$ on a Quadrasorb SI nitrogen adsorption apparatus (Quantachrome, America) by using the Brunner-Emmet-Teller (BET) method.

2.2. General preparation of Ni@N/C catalyst

In a typical synthesis procedure, Ni(II) nitrate hexahydrate (Ni(NO $_3$) $_2$ ·6H $_2$ O), nitrogenous substances, and citric acid (C $_6$ H $_8$ O $_7$) were dissolved in anhydrous ethanol (50 mL) at different ratios. The mixture

was then aged at 70 °C for 4 h under stirring (300 r min⁻¹) until to obtain a greenish gel, followed by drying at 100 °C for 24 h in a drying oven to remove the excess solvent. The obtained greenish solid was then calcined at a fixed bed at 700 °C for 3 h under a high-purity N_2 (99.999%) flow of 40 mL min⁻¹. The heating rate was controlled at 2 °C min⁻¹. The obtained black solids were treated in 1 M H₂SO₄ aqueous solution at 70 °C until the solution was colorless to remove the insecure and uncovered Ni particles. The black solids were then fully washed with deionized water until the pH of the waste solution was 7. Finally, the black solids were dried at -48 °C for 12 h in vacuum by using a freeze dryer. The dried black solids are denoted as Ni@N/C-x, where x is the number of greenish gel, such as Ni@N/C-1.

2.3. Procedure for semi-hydrogenation of alkynes in batch reactor

The reaction was conducted in a stainless-steel autoclave (Anhui Kemi Machinery Technology Co., Ltd., China) with six wells (10 mL per well), one thermocouple, and one circulating water-cooling equipment. Each well has a glass lining, in which were loaded with one 5 mm magnetic stirring bar, 0.5 mmol corresponding terminal alkynes, 5 mg catalyst, and 1 mL solvent. Then, the autoclave was sealed and purged with H₂ three times at 2 MPa pressure and was pressurized with target pressure of H₂. The autoclave was placed into a heating mantle and the stirring rate was set at 300 r min⁻¹. The autoclave was preheated from room temperature to target temperature (inside temperature detected by thermocouple) at the rate of 2 °C min⁻¹. The target temperature was used as the reaction temperature. The reaction proceeded at the reaction temperature for required time. After the reaction, the remaining gas was discharged after the autoclave was cooled down to room temperature. The reaction solutions were collected with a dropper and filtered. The catalyst was immobilized on the magnetic stirring bar and washed thoroughly with ethanol and water. The catalyst (together with magnetic stirring bar) was then dried at -48 °C for 12 h in a vacuum by using a freeze dryer. The reaction products were identified by GC-MS and ¹H NMR and the yields of reaction products were determined by GC with 1,3,5-trimethoxybenzene as internal standard. For ¹H NMR analysis, about 2 mL reaction solutions were concentrated by rotary evaporation and then added with 0.6 mL of CDCl₃ (pre-neutralized with basic Al₂O₃).

2.4. Procedure for the Ni@N/C-1 recycling test in batch reactor

The stability test of Ni@N/C-1 was performed in a stainless-steel autoclave (Anhui Kemi Machinery Technology Co., Ltd., China) with six wells (10 mL per well), one thermocouple, and one circulating water-cooling equipment. The procedure of reaction and product analysis is similar to the S3.1 section. After one batch reaction, the collected catalyst (together with magnetic stirring bar) was thoroughly washed with ethanol and water. The catalyst (together with magnetic stirring bar) was dried at $-48\,^{\circ}\mathrm{C}$ for 12 h in vacuum by using a freeze dryer and was used for the next cycle of reaction.

2.5. Procedure for the Ni@N/C-1 catalyzed semi-hydrogenation of alkynes in flow reactor

The Ni@N/C-1 catalyzed semi-hydrogenation of alkynes was performed in a flow reactor instrument H-Flow-10 (Ou Shi Sheng (Beijing) Technology Co., Ltd., China). Since the catalyst has the magnetic property, 1.2 g of Ni@N/C-1 catalyst is adsorbed on the 10 mm magnet ball, and then filled into the reaction tube; then the entire reaction tube is purged with N_2 , and the entire reaction tube is cleaned with methanol. After that, the reaction tube is heated to a target reaction temperature, and then the hydrogen pressure is set to the pressure of the reaction conditions, and the prepared 0.08 M phenylacetylene methanol solution

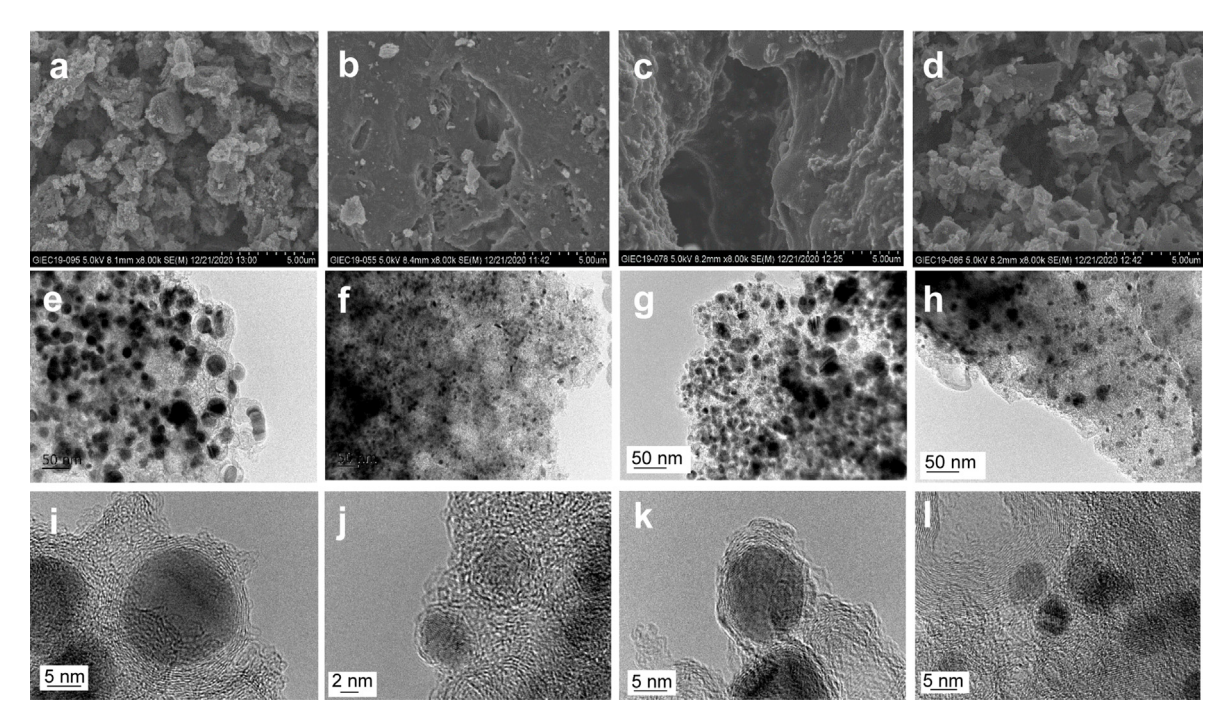


Fig. 1. Representative SEM images of: (a) Ni@N/C-1, (b) Ni@N/C-4, (c) Ni@N/C-5, and (d) Ni@N/C-6; representative HAADF-TEM images of: (e, i) Ni@N/C-1, (f, j) Ni@N/C-4, (g, k) Ni@N/C-5, and (h, l) Ni@N/C-6.

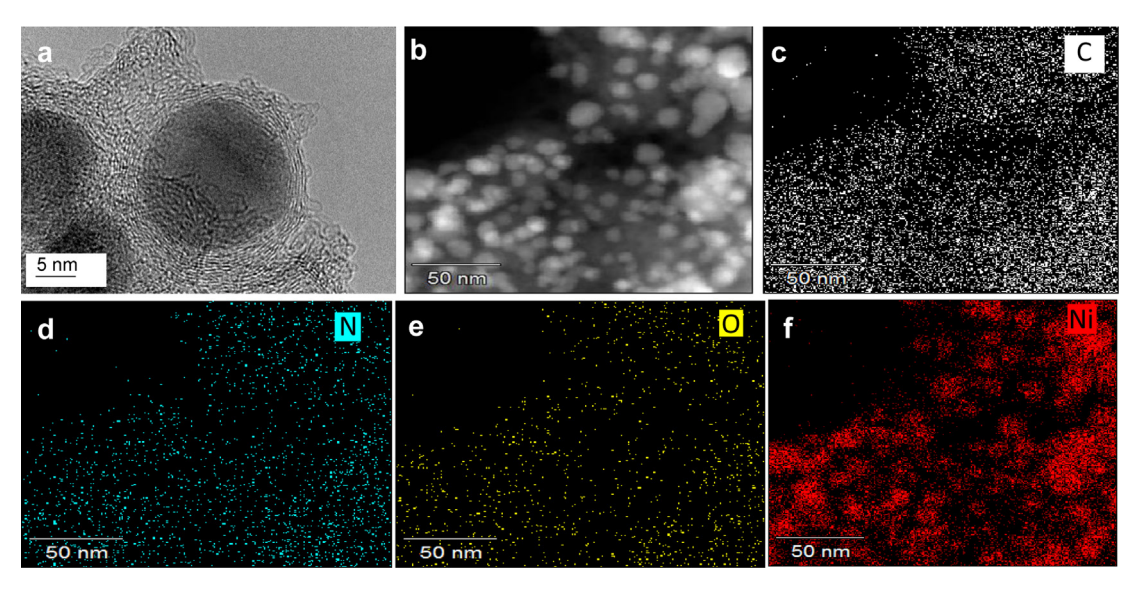


Fig. 2. Representative HAADF-TEM images of: (a) Ni@N/C-1 and (b-f) corresponding EDS element mappings (EFTEM) of gray, C, N, O, and Ni.

is pumped into the reaction tube at a certain flow rate. The reaction solution flows out of the reaction tube while participating in the reaction at the set flow rate in the reaction tube, and then collects the reaction solution for GC sample analysis.

3. Results and discussion

The Ni@N/C catalysts were prepared using our previously reported method with some modifications [41]. Briefly, Ni nitrates, citric acid, and a variety of different amine sources were mixed in EtOH with vigorous stirring. The resulting green gel was dried and calcined, yielding N-doped graphene encapsulated Ni@N/C catalysts. From the representative SEM images and TEM images (Fig. 1), it was noted that different amine sources affected the catalyst's surface significantly. The Ni@N/C-5

catalyst prepared from urea had a dense structure, while the other three catalysts Ni@N/C-1, Ni@N/C-4, and Ni@N/C-6 prepared from melamine, ammonium citrate, and 1,2-propylene diamine respectively had a loose structure which was indicated by the presence of pores. This was further confirmed by the BET measurements of the catalysts. The nitrogen source dramatically affected the size of the metal nanoparticles as shown in Fig. 1e–h. The metal species of Ni@N/C-1 has a uniform size of 12.5 nm, while Ni@N/C-4 prepared using ammonium citrate had the smallest particle size of 5.9 nm. The Ni@N/C-5 catalyst had an uneven metal nanoparticle size, and aggregation of the metal species was observed. The Ni@N/C-6 catalyst prepared using aliphatic amine 1, 2-propylene diamine had an irregular distribution metal particle size. A closer inspection of a selected area on the Ni@N/C catalyst showed the formation of a thin graphene layer structure around Ni. The catalyst

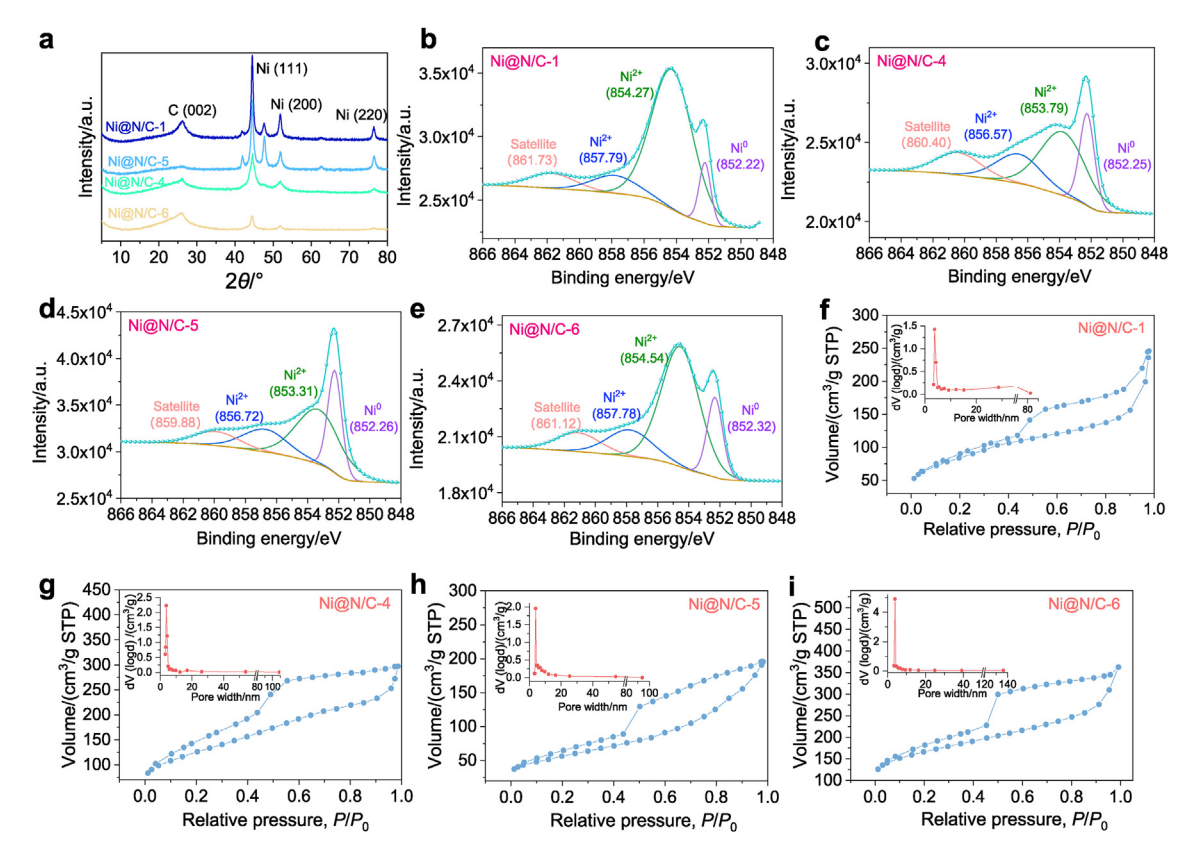


Fig. 3. (a) Representative XRD images of Ni@N/C-1, Ni@N/C-4, Ni@N/C-5, and Ni@N/C-6; representative XPS images of: (b) Ni@N/C-1, (c) Ni@N/C-4, (d) Ni@N/C-5, and (e) Ni@N/C-6; representative BET measurements of N_2 adsorption/desorption isotherm curves and pore size distribution profiles for catalysts (f) Ni@N/C-1, (g) Ni@N/C-4, (h) Ni@N/C-5, and (i) Ni@N/C-6.

prepared using melamine had an obvious thin-layer graphene structure, and the graphene wrapped the active Ni metal with approximately 5 carbon layers. The catalysts Ni@N/C-4 and Ni@N/C-5 were prepared using ammonium citrate or urea as the nitrogen source had less carbon layers. It was observed that the structure of the carbon layers is incomplete, and some carbon layers are destroyed. For the catalyst prepared with 1,2-propanediamine, no obvious carbon-coated metal structure was observed, but the presence of a graphene carbon layer was observed. In addition, the TEM-EDS analysis and high-angle annular dark-field EDS (HAADF-EDS) elemental mapping of Ni@N/C-1 exhibited a very similar distribution, which further indicated the co-existence of both N and Ni species in the Ni@N/C-1 catalyst. The elements of C, N, and O were well dispersed over the Ni nanoparticles according to elemental mappings of the Ni@N/C-1 catalyst, indicating the presence of graphene layers around the nanoparticles. The C, O, N, and Ni atoms are also distributed homogeneously over the other two prepared Ni@C catalysts (Fig. 2 and Fig. S1).

As shown in the XRD profile of different catalysts (Fig. 3a), Ni@N/C-1 had the highest intensity which showed clearly the Ni (111), Ni (200), Ni (220) metal species. Also, the graphene shell C (002) was observed, which agrees with the TEM analysis. The intensity of the peaks for Ni (111), Ni (200), Ni (220) metal species is lower in the Ni@N/C-4 and Ni@N/C-6 catalysts, which indicated that the metal species were dispersed well in the support. It should be noted that nitrogen sources have a great effect on metal dispersion in the graphene support. The catalyst Ni@N/C-4 which was prepared from ammonium citrate had a higher loading of Ni metal, based on SEM-EDS and Inductive Coupled Plasma (ICP) analysis (Tables S2 and S3), and better dispersion than the Ni@N/C-1 catalyst prepared from melamine. The Ni@N/C-6 catalyst, which was prepared from aliphatic amine 1,2-propylenediamine, had the lowest Ni loading of only 8.36% (Table S3). The Ni metal species in this catalyst had a smaller nanoparticle size and better dispersion in the support based on the TEM

analysis. XPS was carried out to elucidate the chemical states of the Ni metal elements (Fig. 3b-e). The survey scan of all the catalysts (Ni@N/C-1,4,5,6) showed the presence of Ni, C, O, and N elements. The trend for Ni@N/C-1 and Ni@N/C-6 catalysts was similar with the presence of metallic Ni⁰ peaks at BE 852.2 eV or 852.3 eV (Ni 2p_{3/2}) after deconvolution. This is lower binding energy than that reported for Ni/AC as well as the N doped Ni/AC-N-0.5 catalysts, which indicated that the strong electron density of the Ni atom in Ni@N/C-1 increased dramatically for the two reported catalysts [42–44]. The other two Ni@N/C-4 and Ni@N/C-5 catalysts also had a similar trend with the presence of metallic Ni⁰ peaks at BE 852.3 eV (Ni 2p_{3/2}) after deconvolution. The presence of a large quantity of high oxidation state Ni²⁺(II) species was also evident by the peaks at BE 854.3-854.5 eV (Ni 2p_{3/2}), BE 856.6-857.7 eV (Ni 2p_{1/2}) and BE 871.3-872.1 eV (Ni 2p_{3/2}). All these observations indicated that the active metal species Ni⁰ were easily oxidized to Ni²⁺(II) during the preparation.

The N 1s spectrum of Ni@N/C-x was recorded between 395.0 eV and 410.0 eV. Deconvolution of the N 1s spectra of Ni@N/C-1 is attributed to the three peaks for the nitrogen species which are assigned to pyridinic-N, pyrrolic-N, and graphitic-N, respectively [28,42,44–46]. This proved that when the N content in the support is increased, the charge transfer from N to Ni intensified. According to the TEM-EDS element analysis, when we changed the nitrogen source from urea to ammonium citrate, to melamine, there was a gradual increase of N content in the catalyst as follows: from Ni@N/C-5 (1.09%), Ni@N/C-4 (1.56%), to Ni@N/C-1 (2.93%). The strong interaction between the N-doped support and Ni, arising from the enhanced electron transfer, improved the stability and activity of the catalyst. When the electron acceptor from the pyridinic-N species interacts with metal atoms, a positive binding energy shift is observed. However, when the graphitic-N species donates electrons to the neighboring metal atoms, there is instead a negative binding energy shift. This increased electron density probably increases the Ni catalyst's

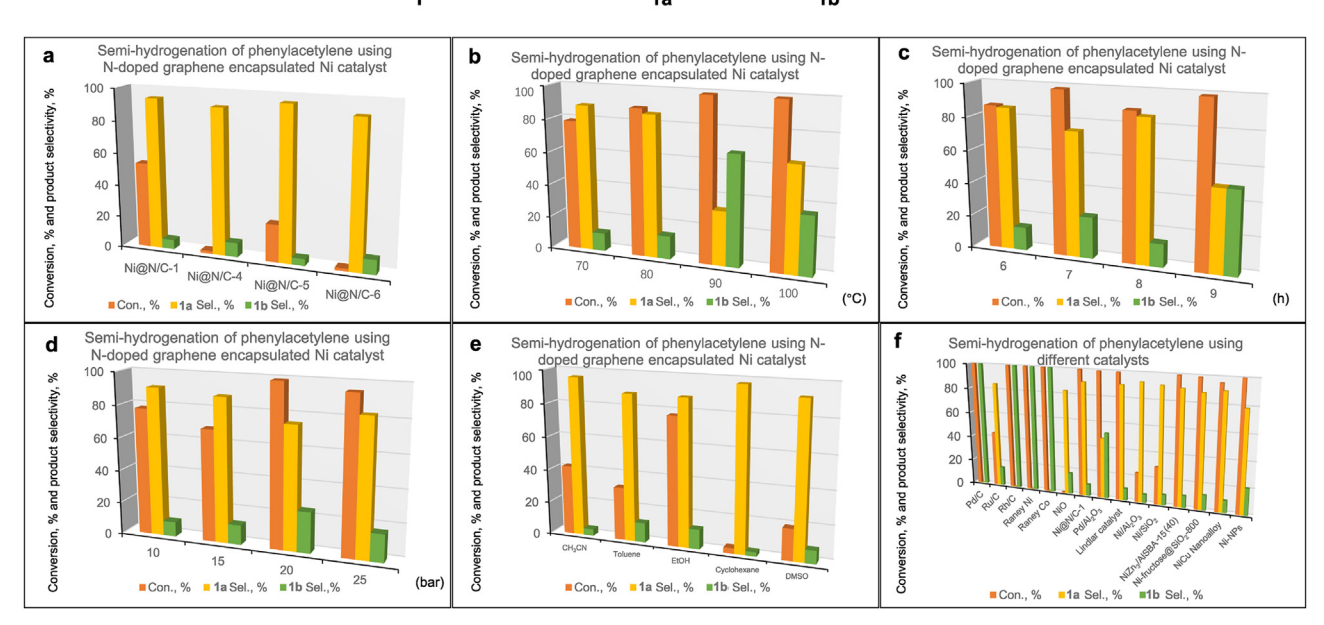


Fig. 4. Optimization of semi-hydrogenation of phenylacetylene using N-doped graphene encapsulated Ni catalyst and comparison to other catalysts. (a) Reaction conditions: 0.5 mmol phenylacetylene, 5 mg catalyst, 4 mL MeOH, 20 bar H₂, r.t., 20 h; (b) Reaction conditions: 0.5 mmol phenylacetylene, 5 mg catalyst, 4 mL MeOH, 20 bar H₂, 80 °C, 6–9 h; (d) Reaction conditions: 0.5 mmol phenylacetylene, 5 mg catalyst, 4 mL MeOH, 10–25 bar H₂, 80 °C, 7 h; (e) Reaction conditions: 0.5 mmol phenylacetylene, 5 mg catalyst, 4 mL MeOH, 10–25 bar H₂, 80 °C, 7 h; (e) Reaction conditions: 0.5 mmol phenylacetylene, 5 mg catalyst, 4 mL MeOH, 20 bar H₂, 80 °C, 7 h; (f) Reaction conditions: Pd/C, Ru/C, Rh/C, Raney Ni, Raney Co, NiO (0.5 mmol phenylacetylene, 5 mg catalyst, 4 mL MeOH, 20 bar H₂, 80 °C, 7 h); Ni@N/C-1 (10 bar H₂, 70 °C, 8 h); Pd/Al₂O₃ (5 wt% phenylacetylene in MeOH, 1 bar H₂, 40 °C, 1.3 h); Lindlar catalyst (5 wt% phenylacetylene in MeOH, 1 bar H₂, 40 °C, 30 h); Ni/Al₂O₃ (5 wt% phenylacetylene in MeOH, 10 wt% Ni loading, 1 bar H₂, 40 °C, 15 h); Ni/SiO₂ (5 wt% phenylacetylene in MeOH, 10 wt% Ni loading, 1 bar H₂, 40 °C, 15 h); Ni-fructose@SiO₂-800 (1 mmol phenylacetylene, 8 mg catalyst (0.6 mol/mol Ni), 2 mL CH₃CN, 10 bar H₂, 110 °C, 5 h); NiCu Nanoalloy (0.005 mol, 50 mg pre-NiCu/MMO, isopropanol, 4 bar H₂, 100 °C, 3 h). Ni-NPs (0.38 mmol phenylacetylene, 10.5 mg Ni(COD)₂ in 0.15 g ionic liquid [CNC₃MMM][NTf₂] prepared *in situ*, 0.5 mL cyclohexane, 4 bar H₂, 30 °C, 3 h). The conversion and selectivity were determined by GC or NMR spectroscopy using an internal standard or as reported in the literature.

selectivity [43,47]. Furthermore, the C 1s electrons are deconvoluted into the four main peaks centered at BE 284.2, 285.7, 286.8, and 288.3 eV, which are assigned to graphitic carbon types: C-C sp², C-C sp³/-C-N, C-O, and C=O, respectively [28,48,49]. To investigate the physical properties of the catalysts surface, we carried nitrogen adsorption studies on a series of Ni@N/C catalyst samples. From the isotherms illustrated in Fig. 3f-3i, it showed that all nitrogen-doped Ni@N/C catalysts have the typical type IV reversible adsorption isotherm curve, indicating a mesoporous surface. The BET surface area of Ni@N/C-1, Ni@N/C-4, Ni@N/C-5, and Ni@N/C-6 was calculated as 297.6, 435.4, 200.7, and 591.9 m^2g^{-1} , respectively (Table S4). The Ni@N/C-5 catalyst prepared from urea had the smallest surface area of 200.7 m² g⁻¹, with the largest pore diameter of 6.03 nm. While catalyst Ni@N/C-6 prepared from aliphatic amine 1,2-propylenediamine, had the largest BET surface area of 591.9 m² g⁻¹ and the smallest average pore diameter of 3.24 nm. Even Ni@N/C-4 catalyst had a higher Ni (32.1%) loading than the Ni@N/C-1 catalyst (25.0%), due to the smaller metal particles and good dispersion, it had a higher BET surface area of 435.4 m² g⁻¹ than the Ni@N/C-1 catalyst (297.6 m² g⁻¹). According to quenched solid density functional theory (QSDFT), the pore-size distribution of these Ni@N/C-1 samples reveals main peaks in the range of approximately 3-5 nm. Based on all these results, we summarized that the most active catalyst, Ni@N/C-1, is characterized by the formation of specific metallic Ni nanoparticles, which are encapsulated in a thin graphene shell.

With the successful development of graphene thin layer encapsulated N-doped catalysts (Ni@N/C-x), our next goal was to investigate their general application for the semi-hydrogenation of challenging terminal alkynes substrates. For this, we chose phenylacetylene as the model

substrate for hydrogenation to optimize the catalysts' activity and reaction conditions. All the prepared N-doped catalysts (Fig. 4a) were evaluated under the standard reaction conditions. Different catalytic reactivity and product selectivity was observed for the hydrogenation of phenylacetylene. The Ni@N/C-1 catalyst gave the best results amongst the catalysts with 53% conversion, 94% selectivity for 1a, and 6% selectivity for the other over-hydrogenated product. The Ni@N/C-4 and Ni@N/C-6 catalysts were not active for the semi-hydrogenation of phenylacetylene under the standard reaction conditions. With the optimized catalyst Ni@N/C-1 in hand, we evaluated the reaction by changing the temperature. The conversion increased from 79% to 99% (Fig. 4b) when the reaction temperature increased from 70 °C to 100 °C, while the selectivity of 1a followed the trend and decreased accordingly. At 80 °C, Ni@N/C-1 catalyzed semi-hydrogenation of phenylacetylene and gave the best results with 92% conversion and 87% selectivity of 1a. Then using this reaction temperature, we evaluated the reaction time to determine the effect of catalytic activity and product distributions. When the reaction time increased from 6 h to 9 h (Fig. 4c), conversion increased from 86% to 99%, but product selectivity decreased from 85% to 50%. When the reaction pressure increased from 10 bar to 25 bar, conversion increased from 78% to 95%, but product selectivity decreased from 91% to 83% (Fig. 4d). Although cyclohexane and CH3CN gave excellent selectivity, the catalyst showed low activity in these solvents (Fig. 4e).

To showcase the generality and selectivity of this novel N-doped graphene layer encapsulated Ni-based nano-catalyst, its reactivity was compared to a few commercially available catalysts such as the Lindlar catalyst, as well as some representative recently reported catalysts [27, 50–52]. The commercial noble catalysts Pd/C, Rh/C, Raney Ni, and

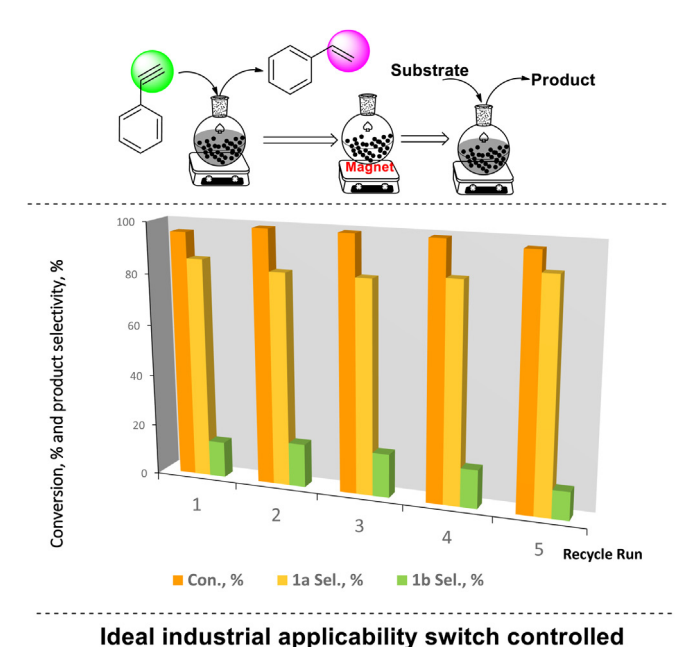
63

99

91

74

Product **b**



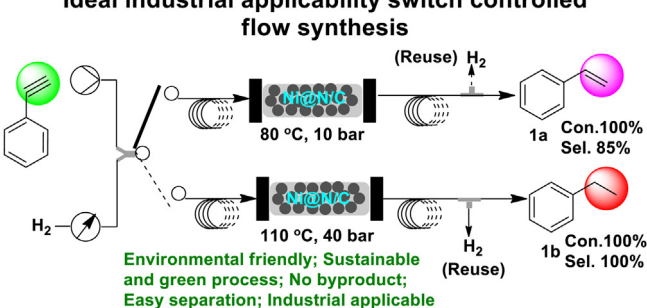


Fig. 5. Catalyst recycle test and ideal flow synthesis of phenylacetylene to prepare different products.

Raney Co (Fig. 4f), which are generally used as hydrogenation catalysts, gave full conversion in the semi-hydrogenation of phenylacetylene but also the over-hydrogenated alkane product. The less active Ru/C catalyst gave 40% conversion and 85% selectivity for 1a. The NiO catalyst was not active for the phenylacetylene semi-hydrogenation under the selected reaction conditions. A slight modification of the reaction conditions (10 bar H2, 70 °C, 8 h), and the Ni@N/C-1 catalyst exhibited excellent reactivity of 99% conversion and comparable selectivity of 91% (Fig. 4f). The prepared Pd/Al₂O₃ catalyst had excellent activity but low selectivity (47.8%) under mild reaction conditions (1 bar H₂, 40 °C, 1.3 h). Although the widely used commercial Lindlar catalyst showed a high selectivity (90.2%) and super activity (99% conversion), the reaction required a long reaction time of up to 30 h. The other two Ni-based catalysts Ni/Al₂O₃ and Ni/SiO₂ showed excellent selectivity (93% and 92%) under 1 bar of H2 pressure and at the mild reaction temperature of 40 °C, they had low activity, with conversions of only 23.5% and 29.8%, respectively, even though the reaction time was prolonged up to 15 h. The reported bi-metal catalysts NiZn₃/AlSBA-15(40), and NiCu nanoalloy gave similar selectivity of 90% for 1a with 99% and 96% conversion respectively under the modified reaction conditions. The in situ prepared Ni-NPs catalyst also gave super reactivity of 100% conversion and moderate selectivity of 79% for 1a with the help of an ionic liquid under mild reaction conditions. Using slightly harsh reaction conditions (10 bar H₂, 110 °C, 5 h), the Ni-fructose@SiO₂-800 catalyst semi-hydrogenated phenylacetylene with 99% conversion and 88% selectivity for 1a.

With these optimized reaction conditions, we then evaluated the substrate scope of the Ni@N/C-1 catalyzed semi-hydrogenation reaction. Under the optimized reaction conditions of 20 bar H₂, 80 °C, 7 h, the

Table 1 Substrate scope of Ni@N/C-1 catalyzed semi-hydrogenation of aromatic alkynes ^a.

 $\underbrace{\text{MeOH, 80 °C, 20 bar H}_2, 7 h} \quad \text{R}^1 \\ \underbrace{\text{R}^2} \quad \text{+} \quad \text{R}^1$

Ni@N/C-1

Entry	Substrate	Product	Con., %	Sel., %
1		la la	99 99	75 91 ^b
2	H ₂ N	H ₂ N	99	87
3	F	2a F 3a	61	85
4	Br	Br	98	84
5	4 5 CI	4a CI 5a CI	99	98
6	O ₂ N 6	O ₂ N 6a	99	89
7	7	7a	43	99
8	но	но	91	73

^aReaction conditions: 0.5 mmol substrate, 5 mg catalyst, 4 mL MeOH, 20 bar H₂,

12a

^bReaction conditions: 0.5 mmol phenylacetylene, 5 mg catalyst, 4 mL MeOH, 10 bar H₂, 70 °C, 8 h.

Ni@N/C-1 catalyst transformed most of the aromatic alkyne substrates to the corresponding target alkene products (Table 1) with excellent conversion and selectivity (exceeds 99%). These results indicate the graphene encapsulated Ni@N/C-1 catalysts' superior application in the field of non-noble heterogeneous catalyzed semi-hydrogenation reactions. The model substrate phenylacetylene gave 99% conversion and product selectivity of 75% for 1a was obtained under the standard reaction conditions. The selectivity for 1a increased to 91% under a slight modification of the reaction conditions. Next, the focus was the electronic effect of the substituent at the meta position on the aromatic alkynes. For substrate 2 with the electron-withdrawing -NH2 group, full conversion of > 99% and 87% selectivity were obtained. Substrate 3 bearing the strongest electron-withdrawing -F group at the meta position was a challenge to semi-hydrogenate and gave only 61% conversion and selectivity of 85% for 3a. For the other two weaker electron-withdrawing -Br and -Cl groups, irrespective of the substituent position, either meta or ortho, the catalyst showed excellent catalytic reactivity and product selectivity. We then examined the effect of changing the substituent at

10

11

12

12

Scheme 2. Graphene encapsulated Ni catalyzed semi-hydrogenation of alkynes.

the para position of the aromatic alkynes. And the substrate $\bf 6$ with the strongest electron-withdrawing -NO₂ group produced product $\bf 6a$ in excellent conversion and good selectivity. The substrate with the strong electron-donating -NMe₂ group also gave excellent conversion of 94% and excellent selectivity of 99%. Substrates with the weak electron-donating t-butyl and N-propyl groups gave only moderated conversion but without any over-hydrogenated products. The graphene encapsulated Ni@N/C-1 catalyst also showed excellent catalytic reactivity of 93% conversion and 74% selectivity for the E isomer product (12a). The electron-withdrawing and electron-donating groups delocalize the electron negativities of the aromatic ring, which further affects the terminal alkynes' electron negativity. The substrates having electron-withdrawing NH₂, Br, Cl, NO₂, and NMe₂ groups gave higher catalytic reactivity and selectivity of the desired semi-hydrogenated product than the substrates with electron-donating t-butyl and N-propyl groups.

A proposed mechanism of graphene encapsulated Ni@N/C catalyzed semi-hydrogenation of alkynes is shown in Scheme 2. First, the molecule H₂ and alkyne substrate are adsorbed on the surface of N-doped Ni@N/C catalyst, the active Ni metal species interact with hydrogen and then the H-H bond is cleaved to give the Ni-H species. Then the Ni-H species make a nucleophilic addition to the C≡C triple bond and produce the alkenyl Nickel intermediate. Finally, when the Ni-C bond of the alkenyl nickel intermediate is broken, the (Z)-olefin product and the recycled Ni catalyst will be produced at the same time. However, since the active metal species Ni⁰ on the Ni catalyst has a strong ability to adsorb hydrogen, and the electron-rich properties of the C=C double bond and benzene ring in the product aromatic olefin, the aromatic olefin and H2 can be again adsorbed on the catalyst active metal species. In this case, the hydrogen is reactivated and Ni-H species are generated, so that the Ni-H species and the C=C double bond in the aromatic olefin undergo a further reductive nucleophilic addition reaction, and finally generate alkane products. Generally speaking, it is quite difficult to control the reaction pathway during the semi-hydrogenation of aromatic alkynes, and the overhydrogenation product alkane usually occurs which decreases the

selectivity and increases the separation problem. Here, however, through the modification of graphene encapsulated Ni catalyst, the ability of the active metal species to adsorb olefins is regulated, thereby avoiding the over-hydrogenation of olefin, and achieving high selectivity and high yield preparation of terminal alkenes from an alkyne.

A stability and recycling test was carried out for the Ni@N/C-1 catalyst in a batch reactor and an advanced flow reactor (Fig. 5). The catalyzed semi-hydrogenation of phenylacetylene using the graphene encapsulated Ni@N/C-1 catalyst did not lose significant reactivity and product selectivity after 5 times recycling test. It should be noted that the stable catalyst with magnetic properties was applied in the industrial flow reactor, and reaction conditions were easily optimized by switching the control valve. The catalyst showed good reactivity and selectivity for the semi-hydrogenation of phenylacetylene in the flow reactor and the catalyst was recovered easily. Semi-hydrogenation catalyzed using graphene encapsulated Ni-based catalysts in a flow reactor was notably environmentally friendly producing less byproduct and easily recycling H₂ for further use. This can provide a feasible reference method for the industrialized selective production of ethylene.

4. Conclusion

In summary, we have reported a successful and facile synthesis of an N-doped thin graphene layer encapsulated Ni-based catalyst. The nitrogen source significantly affected the catalysts' physical properties as well as the interaction between the support and active metal species. This had a further effect on the Ni@N/C catalysts' activity and selectivity for semi-hydrogenation of aromatic alkynes. The optimized Ni@N/C catalyst showed excellent activity and selectivity for semi-hydrogenation of phenylacetylene under mild reaction conditions. More than 10 aromatic alkyne substrates were transformed to the corresponding alkene product with good to excellent reactivity and selectivity. The graphene encapsulated Ni@N/C catalyst also had good stability and has the potential to be applied in an industrial flow reactor for the synthesis of ethylene.

Author contributions

J.-G. L. and L.-L. M. conceived and designed the experiments. J.-G. L., J. M. S., and S.S. L. performed the experiments, analyzed the data, and prepared the Supporting Information. J.-G. L. wrote the paper, T. S. corrected the paper. All authors discussed the results and commented on the manuscript.

Declaration of competing interests

The authors declare that they have no known competing financial interests or personal relationships that could have appeared to influence the work reported in this work.

Acknowledgements

This work was supported financially by the National Natural Science Foundation of China (Project 51976225).

Appendix A. Supplementary data

Supplementary data to this article can be found online at https://doi.org/10.1016/j.gce.2022.01.003.

References

- J.G. de Vries, C.J. Elsevier. The Handbook of Homogeneous Hydrogenation, WILEY-VCH Verlag GmbH & Co. KGaA, Weinheim, Germany, 2006.
- [2] M. Crespo-Quesada, F. Cardenas-Lizana, A.L. Dessimoz, L. Kiwi-Minsker, Modern trends in catalyst and process design for alkyne hydrogenations, ACS Catal. 2 (2012) 1773–1786.
- [3] I.N. Michaelides, D.J. Dixon, Catalytic stereoselective semihydrogenation of alkynes to E-alkenes, Angew. Chem. Int. Ed. 52 (2013) 806–808.
- [4] C. Oger, L. Balas, T. Durand, J.M. Galano, Are alkyne reductions chemo-, regio-, and stereoselective enough to provide pure (Z)-olefins in polyfunctionalized bioactive molecules? Chem. Rev. 113 (2013) 1313–1350.
- [5] J.A. Delgado, O. Benkirane, C. Claver, D. Curulla-Ferre, C. Godard, Advances in the preparation of highly selective nanocatalysts for the semi-hydrogenation of alkynes using colloidal approaches, Dalton Trans. 46 (2017) 12381–12403.
- [6] M.K. Karunananda, N.P. Mankad, E-selective semi-hydrogenation of alkynes by heterobimetallic catalysis, J. Am. Chem. Soc. 137 (2015) 14598–14601.
- [7] B.S. Takale, X. Feng, Y. Lu, M. Bao, T. Jin, T. Minato, Y. Yamamoto, Unsupported nanoporous gold catalyst for chemoselective hydrogenation reactions under low pressure: effect of residual silver on the reaction, J. Am. Chem. Soc. 138 (2016) 10356–10364.
- [8] G. Vile, D. Albani, N. Almora-Barrios, N. Lopez, J. Perez-Ramirez, Advances in the design of nanostructured catalysts for selective hydrogenation, ChemCatChem 8 (2016) 21–33.
- [9] A.J. McCue, A. Guerrero-Ruiz, C. Ramirez-Barria, I. Rodriguez-Ramos, J.A. Anderson, Selective hydrogenation of mixed alkyne/alkene streams at elevated pressure over a palladium sulfide catalyst, J. Catal. 355 (2017) 40–52.
- [10] A.D. Benavidez, P.D Burton, J.L. Nogales, A.R. Jenkins, S.A. Ivanov, J.T. Miller, A.M. Karim, A.K. Datye, Improved selectivity of carbon-supported palladium catalysts for the hydrogenation of acetylene in excess ethylene, Appl. Catal., A 482 (2014) 108–115.
- [11] V.V. Chesnokov, O.Y. Podyacheva, R.M. Richards, Influence of carbon nanomaterials on the properties of Pd/C catalysts in selective hydrogenation of acetylene, Mater. Res. Bull. 88 (2017) 78–84.
- [12] K. Choe, F. Zheng, H. Wang, W. Zhao, G. Xue, X. Qiu, M. Ri, X. Shi, Y. Wang, G. Li, Z. Tang, Fast and selective semihydrogenation of alkynes by palladium nanoparticles sandwiched in metal-organic frameworks, Angew. Chem. Int. Ed. 59 (2020) 3650–3657.
- [13] K. Chernichenko, Á. Madarász, I. Pápai, M. Nieger, M. Leskelä, T. Repo, A frustrated-Lewis-pair approach to catalytic reduction of alkynes to cis-alkenes, Nat. Chem. 5 (2013) 718–723.
- [14] S.P. Desai, J. Ye, J. Zheng, M.S. Ferrandon, T.E. Webber, A.E. Platero-Prats, J. Duan, P. Garcia-Holley, D.M. Camaioni, K.W. Chapman, M. Delferro, O.K. Farha, J.L. Fulton, L. Gagliardi, J.A. Lercher, R.L. Penn, A. Stein, C.C. Lu, Well-defined rhodium-gallium catalytic sites in a metal-organic framework: promoter-controlled selectivity in alkyne semihydrogenation to E-alkenes, J. Am. Chem. Soc. 140 (2018) 15309–15318.
- [15] N. Gorgas, J. Brünig, B. Stöger, S. Vanicek, M. Tilset, L.F. Veiros, K. Kirchner, Efficient Z-selective semihydrogenation of internal alkynes catalyzed by cationic iron (II) hydride complexes, J. Am. Chem. Soc. 141 (2019) 17452–17458.
- [16] B.L. Ramirez, C.C. Lu, Rare-earth supported nickel catalysts for alkyne semihydrogenation: chemo- and regioselectivity impacted by the Lewis acidity and size of the support, J. Am. Chem. Soc. 142 (2020) 5396–5407.

- [17] S.M. Fu, N.-Y. Chen, X.F. Liu, Z.H. Shao, S.-P. Luo, Q. Liu, Ligand-controlled cobaltcatalyzed transfer hydrogenation of alkynes: stereodivergent synthesis of Z- and Ealkenes, J. Am. Chem. Soc. 138 (2016) 8588–8594.
- [18] K. Tokmic, A.R. Fout, Alkyne semihydrogenation with a well-defined nonclassical Co-H₂ catalyst: a H₂ spin on isomerization and E-selectivity, J. Am. Chem. Soc. 138 (2016) 13700–13705.
- [19] K.M. Gramigna, D.A. Dickie, B.M. Foxman, C.M. Thomas, Cooperative H₂ activation across a metal-metal multiple bond and hydrogenation reactions catalyzed by a Zr/ Co heterobimetallic complex, ACS Catal. 9 (2019) 3153–3164.
- [20] Y.L. Wang, Z.D. Huang, Z. Huang, Catalyst as colour indicator for endpoint detection to enable selective alkyne trans-hydrogenation with ethanol, Nat. Catal. 2 (2019) 529–536.
- [21] T. Mitsudome, M. Yamamoto, Z. Maeno, T. Mizugaki, K. Jitsukawa, K. Kaneda, One-step synthesis of core-gold/shell-ceria nanomaterial and its catalysis for highly selective semihydrogenation of alkynes, J. Am. Chem. Soc. 137 (2015) 13452–13455.
- [22] Y. Lu, X.J. Feng, B.S. Takale, Y. Yamamoto, W. Zhang, M. Bao, Highly selective semihydrogenation of alkynes to alkenes by using an unsupported nanoporous palladium catalyst: no leaching of palladium into the reaction mixture, ACS Catal. 7 (2017) 8296–8303.
- [23] X.C. Meng, H.Y. Cheng, Y. Akiyama, Y.F. Hao, W.B. Qiao, Y.C. Yu, F.Y. Zhao, S.-I. Fujita, M. Arai, Selective hydrogenation of nitrobenzene to aniline in dense phase carbon dioxide over Ni/γ-Al₂O₃: significance of molecular interactions, J. Catal. 264 (2009) 1–10.
- [24] V. Polshettiwar, B. Baruwati, R.S. Varma, Nanoparticle-supported and magnetically recoverable nickel catalyst: a robust and economic hydrogenation and transfer hydrogenation protocol, Green Chem. 11 (2009) 127–131.
- [25] K.K. Tanabe, M.S. Ferrandon, N.A. Siladke, S.J. Kraft, G.H. Zhang, J. Niklas, O.G. Poluektov, S.J. Lopykinski, E.E. Bunel, T.R. Krause, J.T. Miller, A.S. Hock, S.T. Nguyen, Discovery of highly selective alkyne semihydrogenation catalysts based on first-row transition-metallated porous organic polymers, Angew. Chem. Int. Ed. 53 (2014) 12055–12058.
- [26] A. Fedorov, H.-J. Liu, H.-K. Lo, C. Coperet, Silica-supported Cu nanoparticle catalysts for alkyne semihydrogenation: effect of ligands on rates and selectivity, J. Am. Chem. Soc. 138 (2016) 16502–16507.
- [27] Y. Liu, J.Y. Zhao, J.T. Feng, Y.F. He, Y.Y. Du, D.Q. Li, Layered double hydroxide-derived Ni-Cu nanoalloy catalysts for semi hydrogenation of alkynes: improvement of selectivity and anti-coking ability via alloying of Ni and Cu, J. Catal. 359 (2018) 251–260.
- [28] G. Jaiswal, V.G. Landge, M. Subaramanian, R.G. Kadam, R. Zbořil, M.B. Gawande, E. Balaraman, N-graphitic modified cobalt nanoparticles supported on graphene for tandem dehydrogenation of ammonia-borane and semihydrogenation of alkynes, ACS Sustain. Chem. Eng. 8 (2020) 11058–11068.
- [29] X. Shi, X. Wen, S. Nie, J. Dong, J. Li, Y. Shi, H. Zhang, G. Bai, Fabrication of Ni₃N nanorods anchored on N-doped carbon for selective semi-hydrogenation of alkynes, J. Catal. 382 (2020) 22–30.
- [30] I. Lee, J.B. Joo, Y.D. Yin, F. Zaera, A yolk@shell nanoarchitecture for Au/TiO₂ catalysts, Angew. Chem. Int. Ed. 50 (2011) 10208–10211.
- [31] J.P. Holgado, F. Ternero, V.M. Gonzalez-delaCruz, A. Caballero, Promotional effect of the base metal on bimetallic Au-Ni/CeO₂ catalysts prepared from core-shell nanoparticles, ACS Catal. 3 (2013) 2169–2180.
- [32] Z.W. Li, L.Y. Mo, Y. Kathiraser, S. Kawi, Yolk-satellite-shell structured Ni-yolk@Ni@ SiO₂ nanocomposite: superb catalyst toward methane CO₂ reforming reaction, ACS Catal. 4 (2014) 1526–1536.
- [33] S.K. Movahed, N.F. Lehi, M. Dabiri, Palladium nanoparticles supported on coreshell and yolk-shell Fe₃O₄@nitrogen doped carbon cubes as a highly efficient, magnetically separable catalyst for the reduction of nitroarenes and the oxidation of alcohols, J. Catal. 364 (2018) 69–79.
- [34] C.V.S. Almeida, G. Tremiliosi, K.I.B. Eguiluz, G.R. Salazar-Banda, Improved ethanol electro-oxidation at Ni@Pd/C and Ni@PdRh/C core-shell catalysts, J. Catal. 391 (2020) 175–189.
- [35] J. Gao, R. Ma, L. Feng, Y.F. Liu, R. Jackstell, R.V. Jagadeesh, M. Beller, Ambient hydrogenation and deuteration of alkenes using a nanostructured Ni-Core-Shell catalyst, Angew. Chem. Int. Ed. 60 (2021) 18591–18598.
- [36] S. Kim, J. Lauterbach, E. Sasmaz, Yolk-shell Pt-NiCe@SiO₂ single-atom-alloy catalysts for low-temperature dry reforming of methane, ACS Catal. 11 (2021) 8247–8260.
- [37] A.K. Geim, K.S. Novoselov, The rise of graphene, Nat. Mater. 6 (2007) 183-191.
- [38] A.H. Castro Neto, F. Guinea, N.M.R. Peres, K.S. Novoselov, A.K. Geim, The electronic properties of graphene, Rev. Mod. Phys. 81 (2009) 109–162.
- [39] D.L. Wong, K.P. Nuckolls, M. Oh, B. Lian, Y.L. Xie, S.J. Jeon, K. Watanabe, T. Taniguchi, B.A. Bernevig, A. Yazdani, Cascade of electronic transitions in magicangle twisted bilayer graphene, Nature 582 (2020) 198–202.
- [40] J.M. Park, Y. Cao, K. Watanabe, T. Taniguchi, P. Jarillo-Herrero, Tunable strongly coupled superconductivity in magic-angle twisted trilayer graphene, Nature 590 (2021) 249–255.
- [41] J.G. Liu, Y.T. Zhu, C.G. Wang, T. Singh, N. Wang, Q.Y. Liu, Z.B. Cui, L.L. Ma, Facile synthesis of controllable graphene-co-shelled reusable Ni/NiO nanoparticles and their application in the synthesis of amines under mild conditions, Green Chem. 22 (2020) 7387–7397.
- [42] C. Guimon, A. Auroux, E. Romero, A. Monzon, Acetylene hydrogenation over Ni-Si-Al mixed oxides prepared by sol-gel technique, Appl. Catal., A 251 (2003) 199–214.
- [43] L. Wang, F.X. Li, Y.J. Chen, J.X. Chen, Selective hydrogenation of acetylene on SiO₂supported Ni-Ga alloy and intermetallic compound, J. Energy Chem. 29 (2019) 40–49.

- [44] Z. Xu, S. Zhou, M. Zhu, Ni catalyst supported on nitrogen-doped activated carbon for selective hydrogenation of acetylene with high concentration, Catal. Commun. 149 (2021) 106241.
- [45] H.W. Liang, W. Wei, Z.S. Wu, X.L. Feng, K. Mullen, Mesoporous metal-nitrogen-doped carbon electrocatalysts for highly efficient oxygen reduction reaction, J. Am. Chem. Soc. 135 (2013) 16002–16005.
- [46] W. Xiong, Z.N. Wang, S.L. He, F. Hao, Y.Z. Yang, Y. Lv, W.B. Zhang, P.L. Liu, H.A. Luo, Nitrogen-doped carbon nanotubes as a highly active metal-free catalyst for nitrobenzene hydrogenation, Appl. Catal., B 260 (2020) 118105.
- [47] Y. Chen, J. Chen, Selective hydrogenation of acetylene on SiO₂ supported Ni-In bimetallic catalysts: promotional effect of In, Appl. Surf. Sci. 387 (2016) 16–27.
- [48] J.Y. Liu, H.Y. Chang, Q.D. Truong, Y.C. Ling, Synthesis of nitrogen-doped graphene by pyrolysis of ionic-liquid-functionalized graphene, J. Mater. Chem. C 1 (2013) 1713–1716.
- [49] G. Greczynski, L. Hultman, Compromising science by ignorant instrument calibration-need to revisit half a century of published XPS data, Angew. Chem. Int. Ed. 59 (2020) 5002–5006.
- [50] H. Konnerth, M.H.G. Prechtl, Selective partial hydrogenation of alkynes to (Z)-alkenes with ionic liquid-doped nickel nanocatalysts at near ambient conditions, Chem. Commun. 52 (2016) 9129–9132.
- [51] K. Murugesan, A.S. Alshammari, M. Sohail, M. Beller, R.V. Jagadeesh, Monodisperse nickel-nanoparticles for stereo- and chemoselective hydrogenation of alkynes to alkenes, J. Catal. 370 (2019) 372–377.
- [52] L. Yang, S.Y. Yu, C. Peng, X.C. Fang, Z.M. Cheng, Z.M. Zhou, Semihydrogenation of phenylacetylene over nonprecious Ni-based catalysts supported on AlSBA-15, J. Catal. 370 (2019) 310–320.